Electronic Supplementary Material (ESI) for Inorganic Chemistry Frontiers.
This journal is © the Partner Organisations 2024

Supporting Information

γ-Fe_2O_3 Decorating N, S Co-doped Carbon Nanosheet as Cathode Electrocatalyst toward Different-scenario Fuel Cell

Xintao Zhou [a,c], Mingyang Wu [c], Kai Chen [b], Haijian Wang [c], Zhenhai Wen [b, c*], Suqin Ci [a*]

a Fujian Provincial Key Laboratory of Soil Environmental Health and Regulation, College of Resources and Environment, Fujian Agriculture and Forestry University, Fuzhou 350002, China

b CAS Key Laboratory of Design and Assembly of Functional Nanostructures, and Fujian Provincial Key Laboratory of Materials and Techniques toward Hydrogen Energy, Fujian Institute of Research on the Structure of Matter, Chinese Academy of Sciences, Fuzhou, Fujian, 350002, China

c Key Laboratory of Jiangxi Province for Persistent Pollutants Control, National-Local Joint Engineering Research Center of Heavy Metals Pollutants Control and Resource Utilization and Resources Recycle, Nanchang Hangkong University, Nanchang, 330063, Jiangxi, China

** Corresponding authors*

E-mail: wen@fjirsm.ac.cn, sqci@fafu.edu.cn

1. Electrochemical measurements

All electrochemical measurements were performed on a conventional three-electrode system with using CHI 760E electrochemical workstation (Shanghai Chenhua, China) at room temperature, working electrode (glassy carbon electrode (GCE, 3 mm diameter), rotating disk electrode (RDE, 4 mm diameter), rotating ring disk electrode (RRDE, inner diameter of 5 mm and an outer diameter of 7 mm), reference electrode (Hg/HgO or Ag/ AgCl) and counter electrode (Pt wire), respectively. The GCE was polished with 1.0, 0.3 and 0.05 μm alumina powder respectively and rinsed by deionized water for further use.

Treatment of working electrode: 10 mg of catalyst, 840 μL of water, 100 μL of Nafion solution and 60 μL of ethanol were mixed, and then placed in an ultrasonic cleaner for 0.5 h to form a homogeneous ink. Drop 6 μL of ink on the working electrode and dry at room temperature for later use. All of the potentials were calibrated to the RHE based on the equation (1):

$$E\ vs.\ RHE = E\ vs.\ Ag/AgCl + 0.059\ pH + 0.197\ V \quad (1)$$

The electron transfer number (n) was determined by the following equation (2):

$$n = 4 * ID\ (I\ D + IR/N) \quad (2)$$

Where ID is the disk current and IR is the ring current a speed of 1600 rmp, N is the collection efficiency of Pt ring (N=0.37).

H_2O_2 selectivity of the resultant samples can be calculated by the following equation (3):

$$H_2O_2\% = (200\ I_R/N)/\ (I_D + I_R\ /N) \quad (3)$$

2. Assemble and test of Rechargeable Zn-air Batteries (RZABs)

Typically, Zn-air battery was tested in a self-made electrochemical device. Zn foil was used as metal electrode, the catalysts-loading carbon paper was as air electrode, and the electrolyte with a mixed solution of 6 M KOH and 0.2 M zinc acetate. The catalyst ink was prepared by dispersing 10 mg catalysts into a mixed solution of 900 μL of ethanol, 100 μL of water and 40 μL of Nafion (5 *wt* %), followed by ultrasonically treated for 20 min. The catalyst ink was repeatedly dropped on the carbon paper to achieve the mass loading of 1.0 mg cm^2. The performance of RZABs were measured on a CHI 760E electrochemical workstation and

LAND-CT2001A test system. The specific capacity was calculated according to the equation (4)

$$Csp = (i^* t) / m_{Zn} \quad (4)$$

Where i is the applied current (mA), t is service time (h), and mZn represents the mass of consumed zinc (g).

3. Operation and configuration of Microbial Fuel Cells (MFCs)

Take 20 mg of catalyst, 25 μL of Nafion solution, 125 μL of deionized water, and 50 μL of absolute ethanol in a centrifuge tube for 0.5 h to form a uniformly dispersed catalyst ink. Then evenly spread the catalyst ink on both sides of carbon cloth (1 cm × 2 cm), and fix the carbon cloth on the titanium wire, then the cathode electrode is successfully prepared. In this paper, a traditional two-chamber MFCs reaction vessel is used, and the volume of each vessel is about 150 mL. The two reaction vessels are separated by a proton exchange membrane (PEM, Membrane International Inc., Ringwood, NJ, USA), and then fix the two reaction vessels with clamps to build the reaction. The electricity-producing microorganisms in the experiment originated from the sludge of a sewage treatment plant (Xianghu Sewage Treatment Plant in Nanchang City, Jiangxi Province). In order to fairly compare the oxygen reduction performance of cathode catalysts in MFCs, the cathode catalysts to be compared can be installed in the same cathode chamber and connected to the same anode.

Every 5 minutes, use a digital multimeter (2700, Keithley Instruments, Inc., Cleveland, OH) to record the battery voltage and cathode potential at both ends of the external circuit. A potentiostat (Reference 600, Gamry Instruments, Warminster, PA) is used to obtain the polarization curve at a scan rate of 0.5 mV s^{-1}. The maximum power/current density is calculated by normalizing the cathode surface area.

2. DFT Details

2.1 DFT parameters

Spin-polarized DFT calculations were performed with periodic super-cells under the generalized gradient approximation (GGA) using the Perdew-Burke-Ernzerhof (PBE) functional for exchange-correlation and the ultrasoft pseudopotentials for nuclei and core

electrons. The Brillouin-zones were sampled with 2×2×2 for structure optimization and 2×2×1 for dos and spin density calculation. The PWSCF codes contained in the Quantum ESPRESSO distribution1 were used to implement the calculations.[1]

2.2 ORR calculation details

Since ORR is the reversed reaction of OER. We used computational hydrogen electrode (CHE) method to get the FED.

2.3. Virtual energetic span as the activity determining term

Norskov's approach uses the largest Gibbs energy (ΔG max) as the activity determining term. This descriptor is proposed under the assumption of so-called "rate determining step assumption": the slowest step should control the total kinetic of a series process. [2] However, for a multi-step reaction that takes place at limited position, such as catalytic reaction, it has been gradually noticed in last ten years that there is no such thing of a "rate determining step" (RDS), instead, there should be a "rate determining state".[3]That is, the catalytic activity should be co-determined by several steps. Based on such idea, one should avoid use ΔG^{max}, but to build some newly proposed descriptor that abandon the using of rds. There are now two such kinds of descriptors, one is the highest free energy of an reaction intermediate (denoted as G_{max} (RI)) proposed by Exner et al.[4] And we will use the latter as the activity determining term in this paper. The "virtual energetic span" (δE^{v}) comes from the "energetic span" that proposed by Kozuch et al. [5] It is the simplification of the result of a full microkinetic model. Here we only give its brief conclusion: to use the virtual energetic span, we can still follow the basic principle of Norskov's method, to build a TS-free FED. What is different from Norskov's approach is we can treat the mid-point of each joint line in FED, as the "virtual transition states (TS^{v})". We name it virtual transition state because it is not the real energy of the transition state, but it has a constant difference to the real energy of the transition state. This can strictly prove under the method of Norksov.

2.4 Comparing with other mechanisms of ORR

According to more traditional knowledge, the ORR can be separated into the associative and dissociative mechanisms. Associative mechanism is more familiar, while dissociative

mechanism is much less mentioned. For dissociative mechanism, the reaction formulas are written as:

$O_2(aq)+*\rightarrow O*+O*$

$2O*+H^{+}+e\rightarrow OH*+O*$

$O*+OH*+ H^{+}+e\rightarrow H_2O\ (aq)+O*$

$O*+H_{+}+e\rightarrow OH*$

$OH*+ H_{+}+e\rightarrow H_2O\ (aq)+*$

Besides that, literature has also reported other two possible pathways for the associative mechanism mentioned. The first is to bypass the fielding of OOH*, but to generate O* and OH*, that is

$O_2+ H^{+}+e+2*\rightarrow O*+OH*$ dis1

This step can be proceeded by two steps, which is the second pathways:[6]

$O_2+ H^{+}+e+*\rightarrow OOH*$

$OOH*\rightarrow O*+OH*$ dis2

Those steps, in addition of the possible desorption of H_2O*, and adsorption of O_2*, can generate 16 possible pathways. The preference for pathway should depend on some macro properties of material such as diffusion, steric effect and so on.

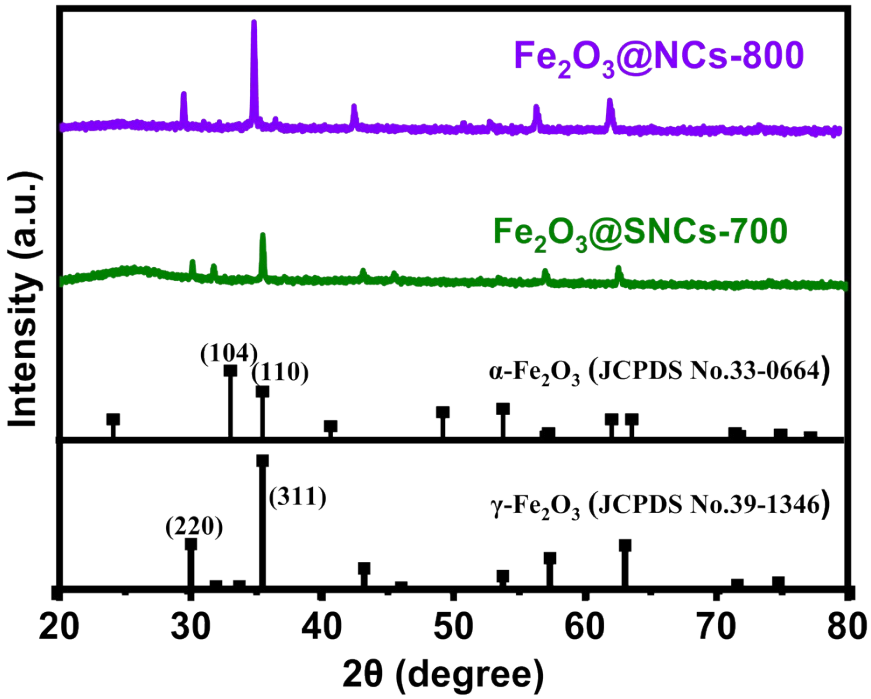

Figure S1. XRD pattern for Fe_2O_3@NCs-800 and Fe_2O_3@SNCs-700.

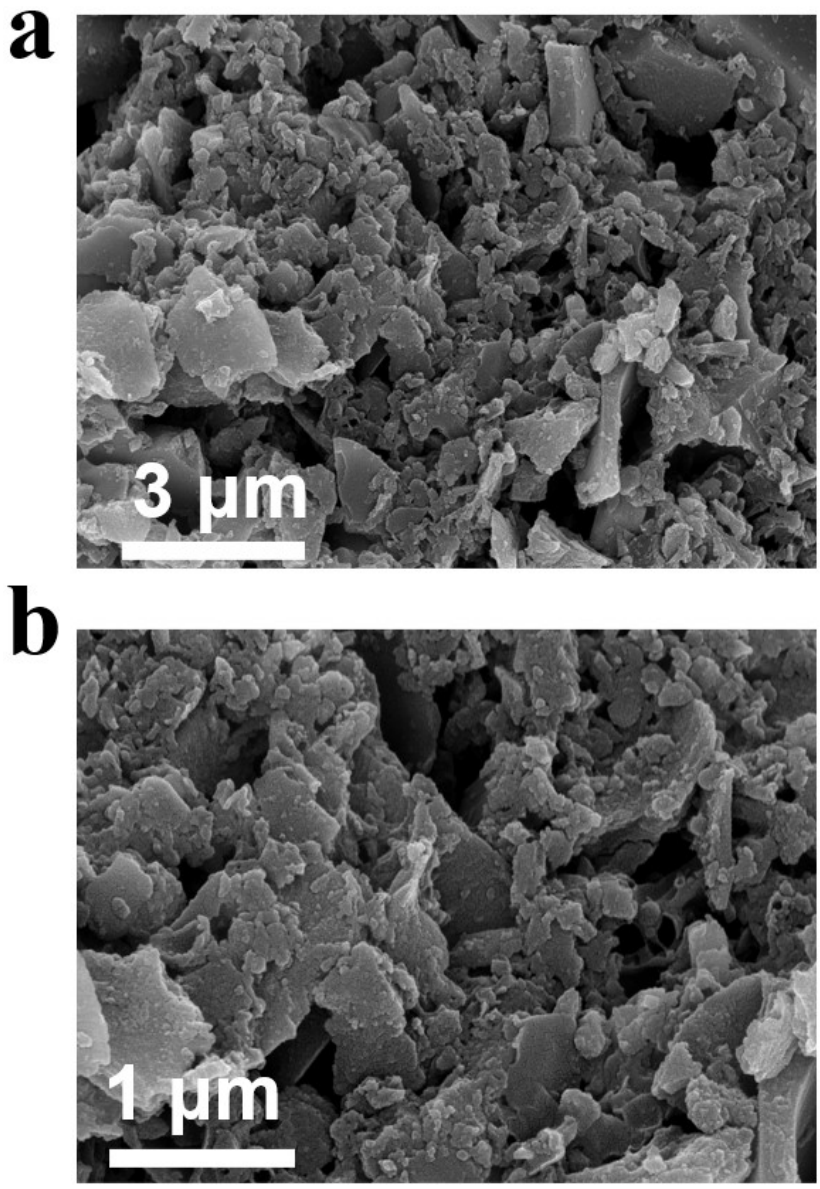

Figure S2.SEM images of Fe_2O_3@NCs-800.

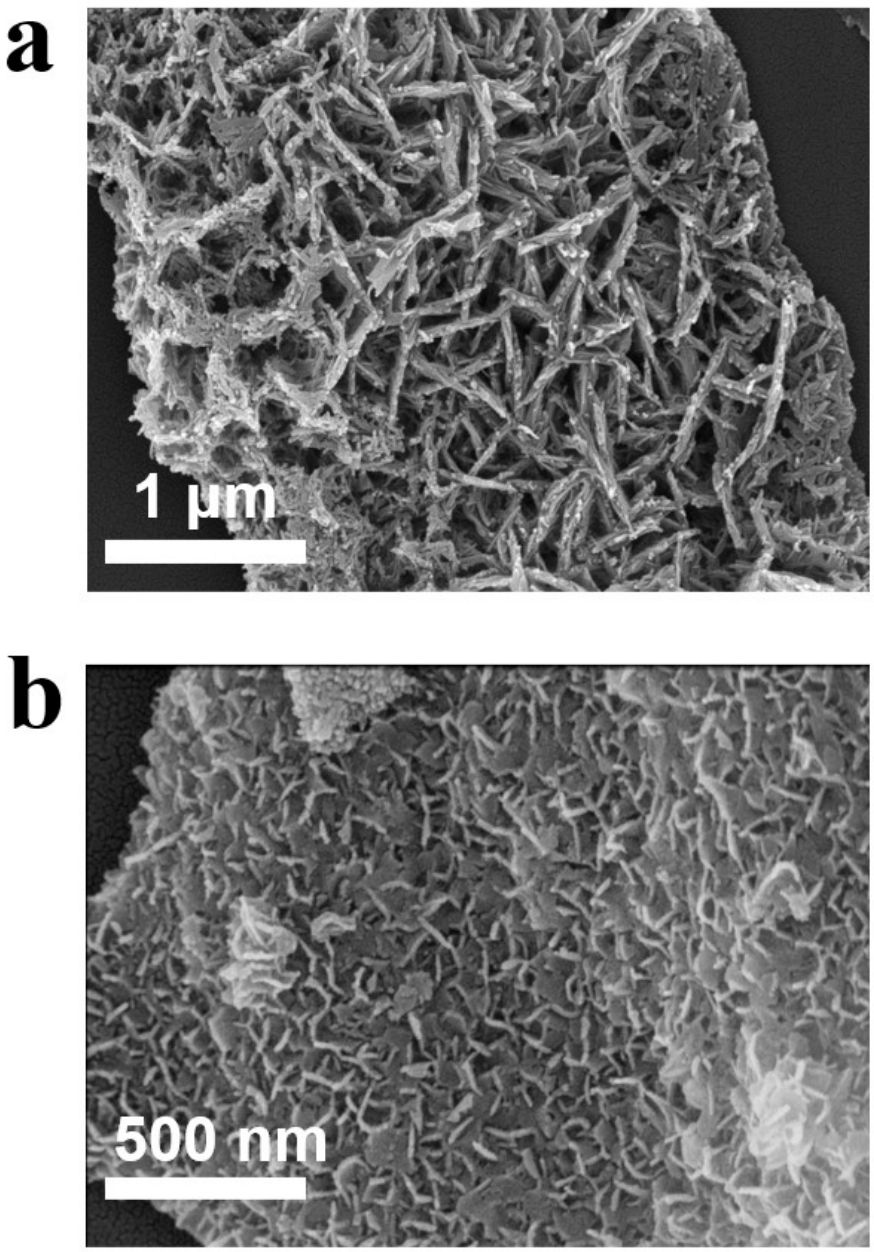

Figure S3. SEM images of Fe_2O_3@SNCs-700.

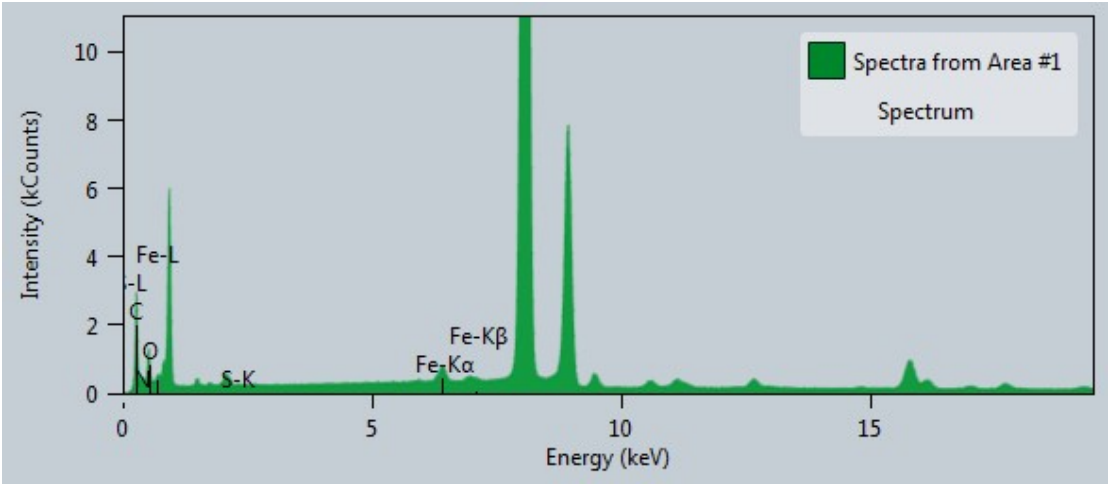

Figure S4.EDS energy spectrum of Fe_2O_3@SNCs-800.

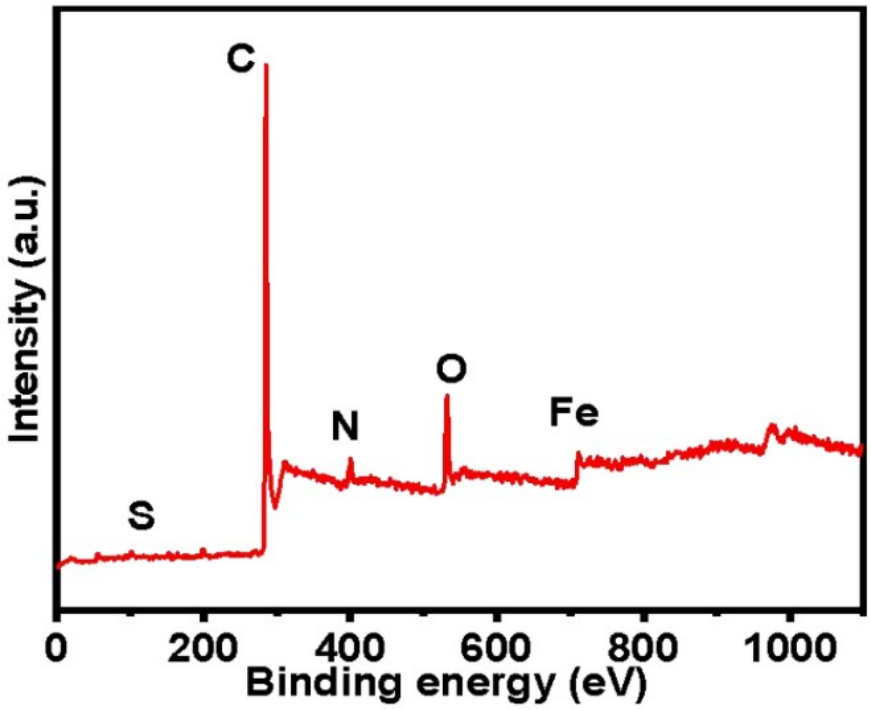

Figure S5. XPS surface survey of γ-Fe_2O_3@SNCs-800.

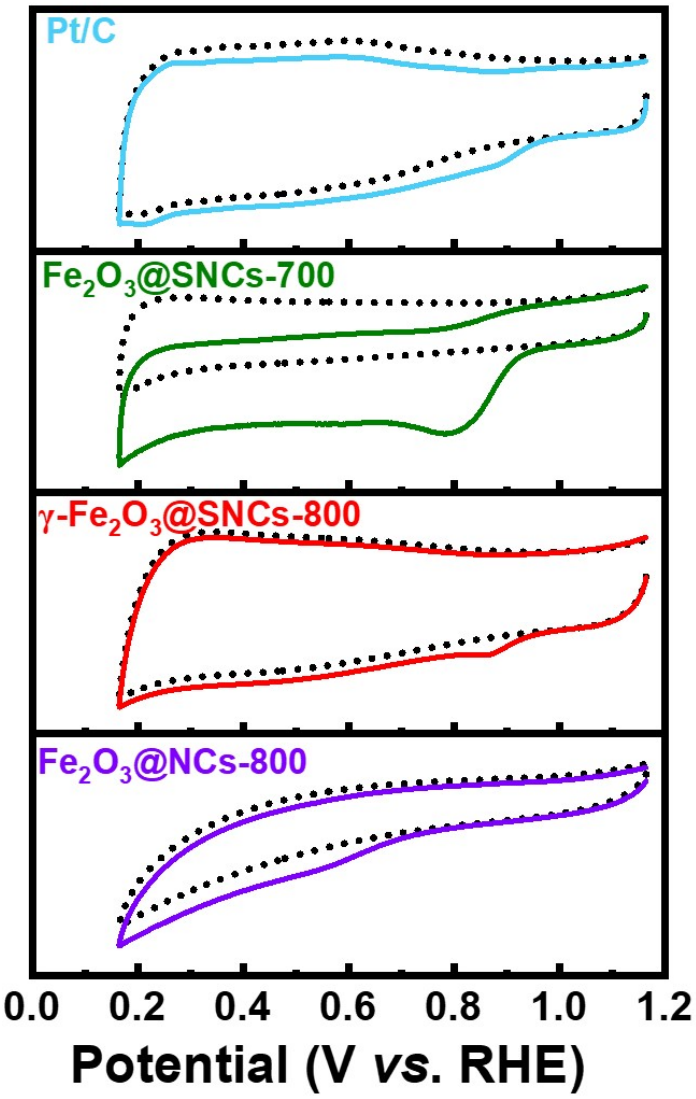

Figure S6. CV curves N_2-saturated and O_2-saturated 0.1 mol L^{-1} KOH with a scan rate of 10 mV s^{-1}.

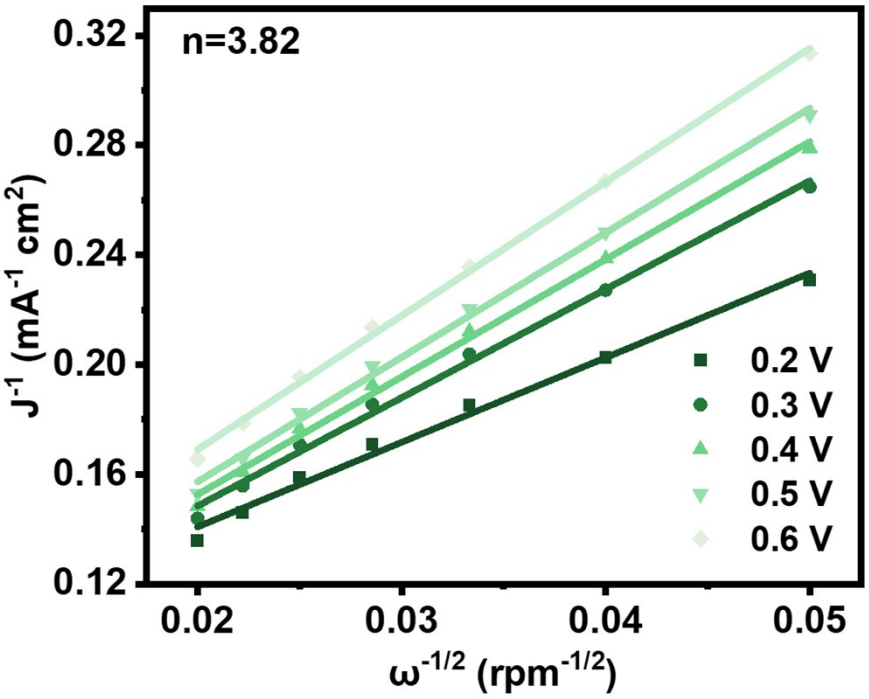

Figure S7. K-L curves of γ-Fe_2O_3@SNCs-800 catalyst in 0.1 M KOH.

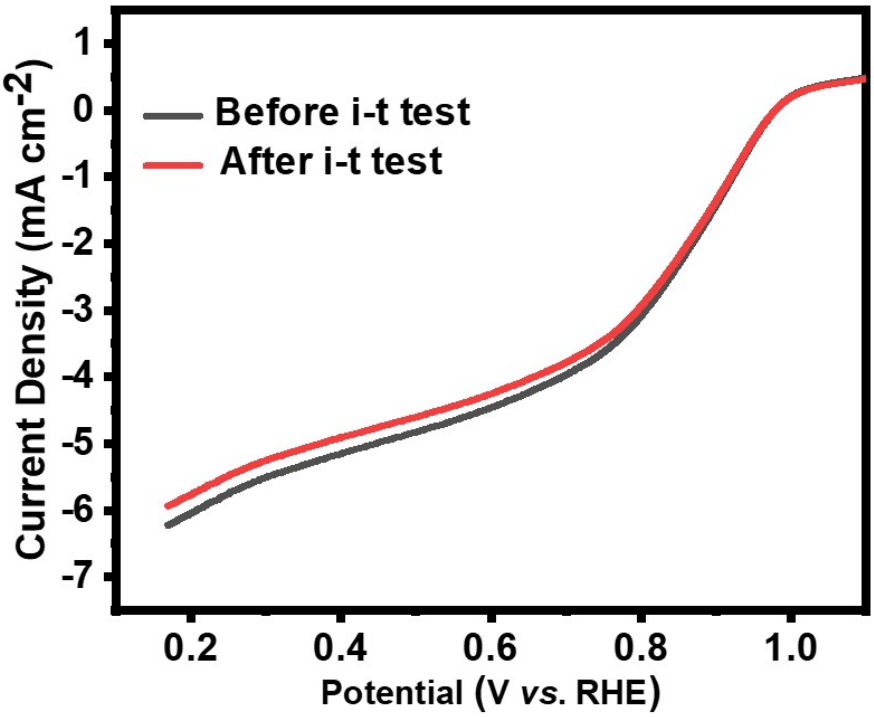

Figure S8. Before/after i-t stability test of γ-Fe_2O_3@SNCs-800 LSV curves in 0.1 M KOH.

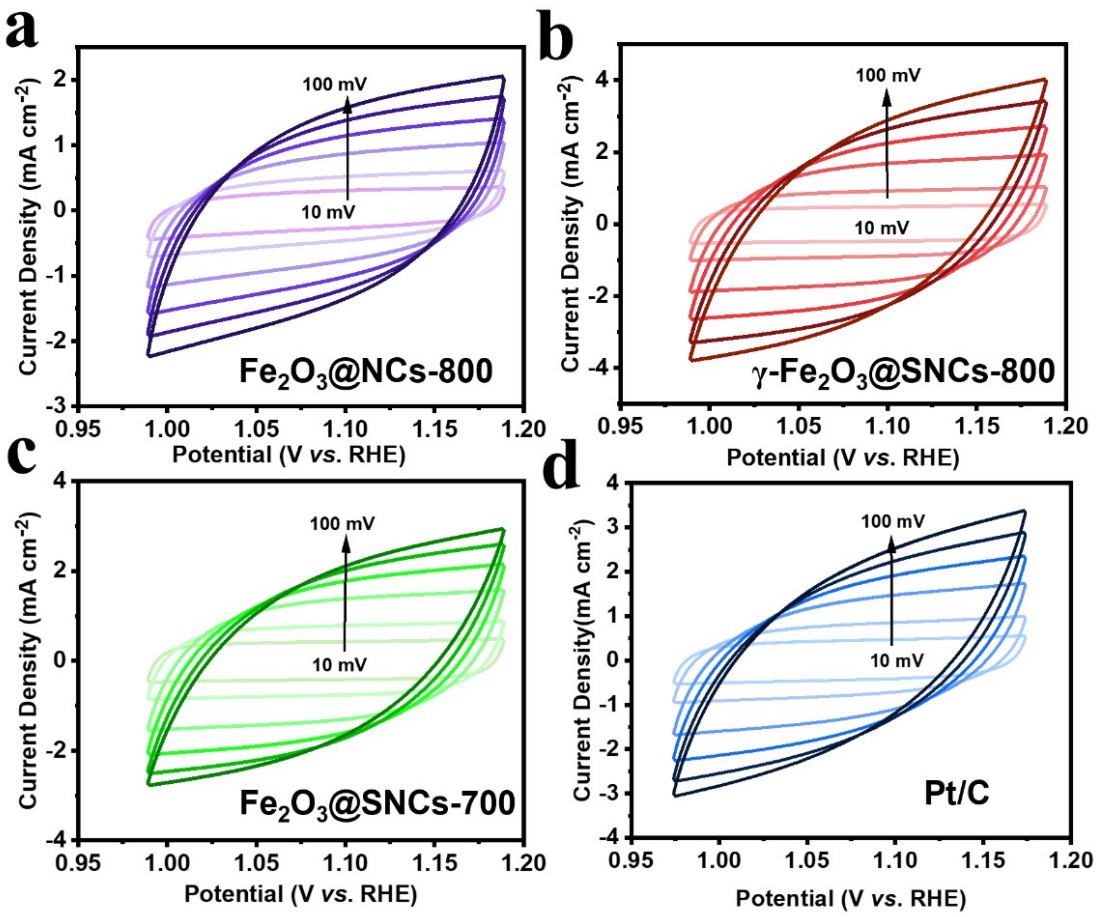

Figure S9. The CVs curves for ORR C_{dl} at different scan rates of (a) Fe_2O_3@NCs-800; (b) γ-Fe_2O_3@SNCs-800; (c) Fe_2O_3@SNCs-700 and (d) Pt/C.

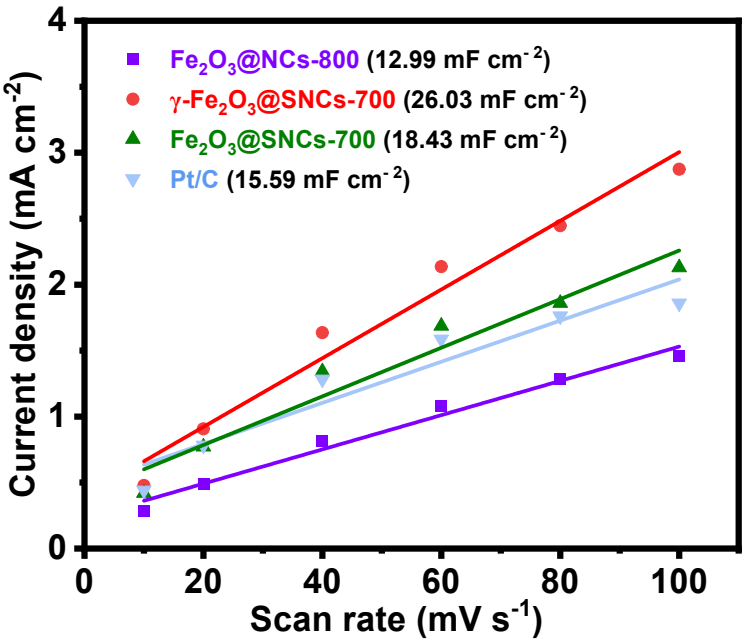

Figure S10. The linear fitting of scan rates with capacitive current densities for ORR.

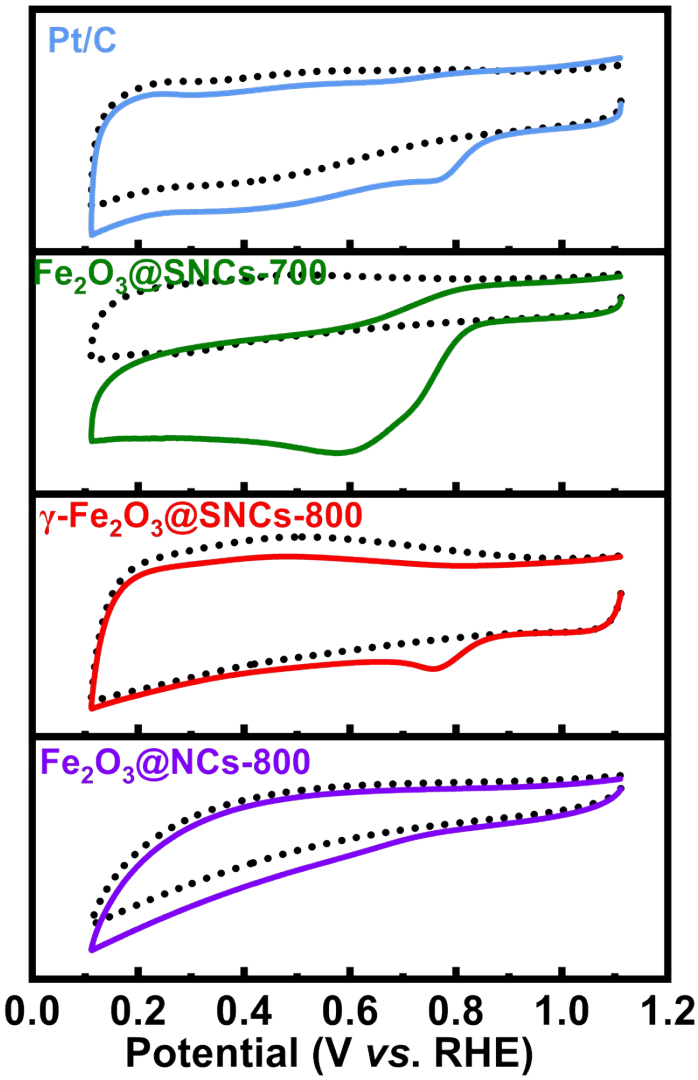

Figure S11. (a) CV curves in N_2-saturated and O_2-saturated with a scan rate of 10 mV s^{-1} in 0.1 M PBS.

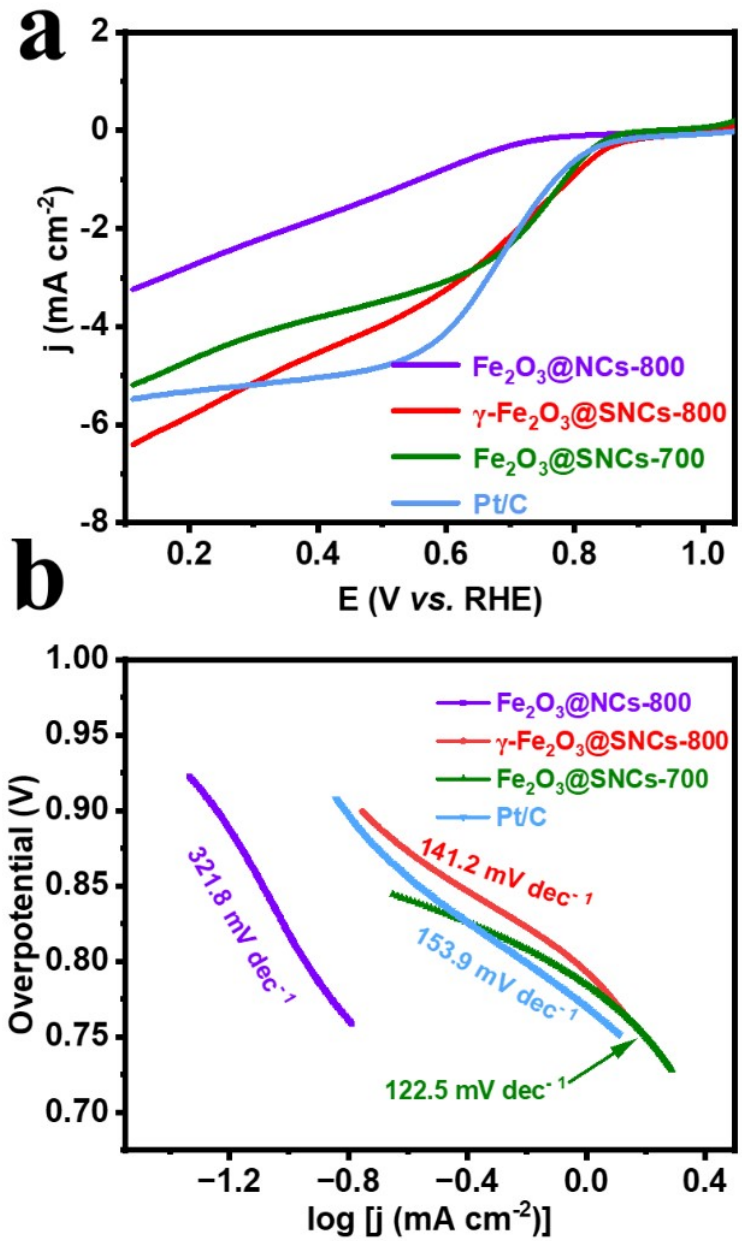

Figure S12. (a) LSV of each catalyst (1600 rpm); (b) Tafel slope curve of each catalyst of Fe_2O_3@SNCs-800 in 0.1 M PBS.

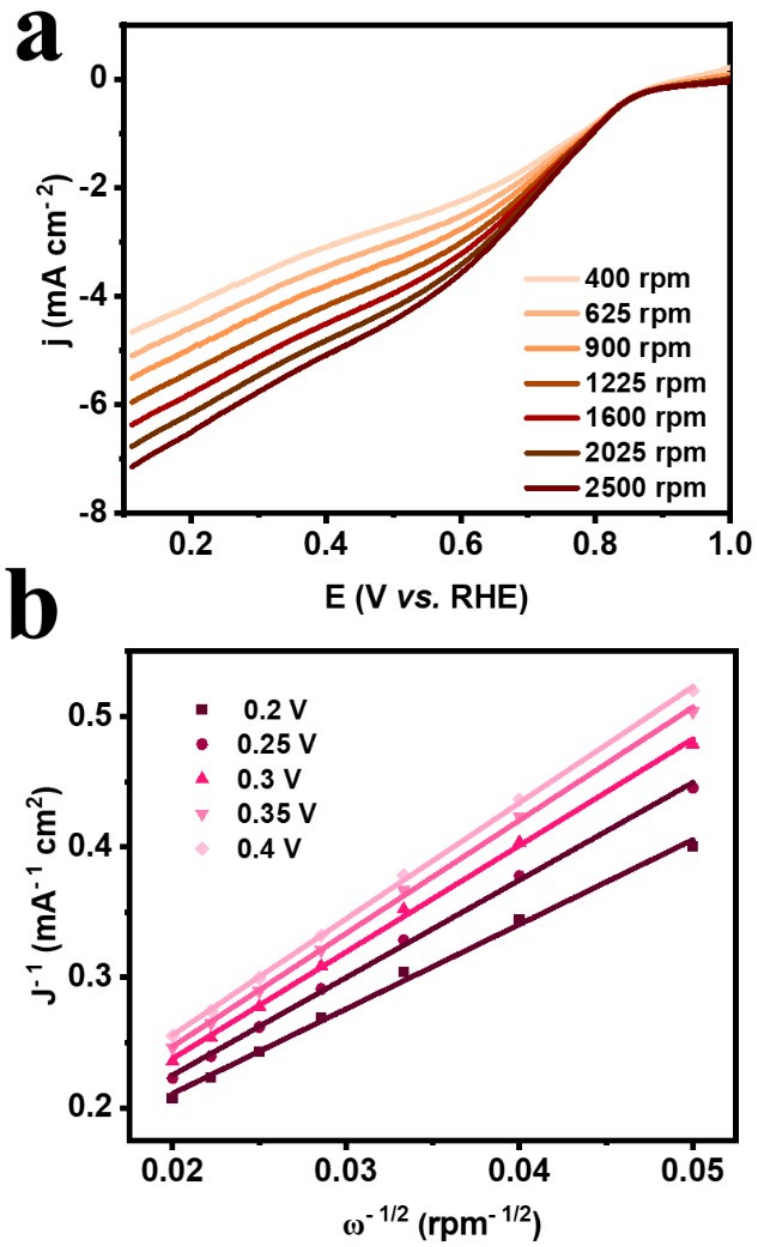

Figure S13. (a) LSV and (b) K-L curves of γ-Fe_2O_3@SNCs-800 catalyst in 0.1 M PBS.

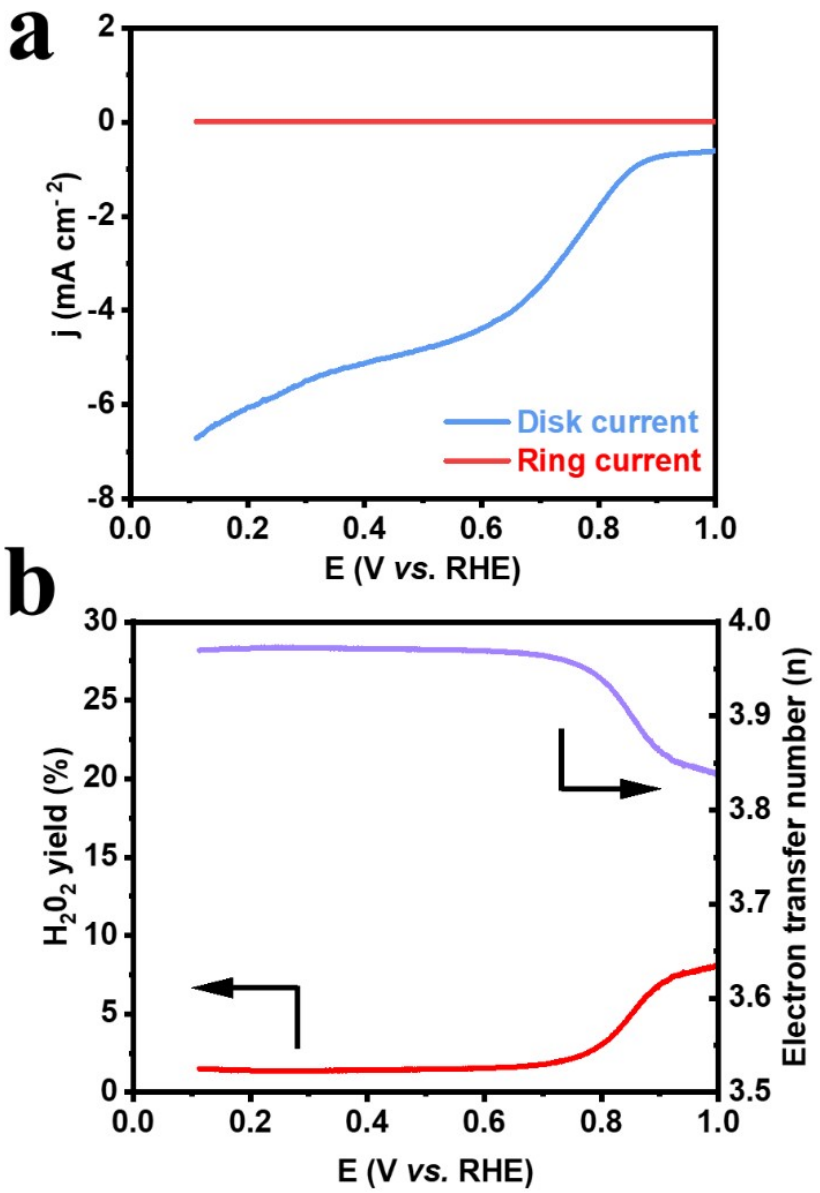

Figure S14. (a) Ring current and disk current of γ-Fe_2O_3@SNCs-80catalyst (1600 rpm, 1.45 V *vs.* RHE) in 0.1 M PBS; (b) Electron transfer number and H_2O_2 yield of γ-Fe_2O_3@SNCs-800 catalyst in 0.1 M PBS.

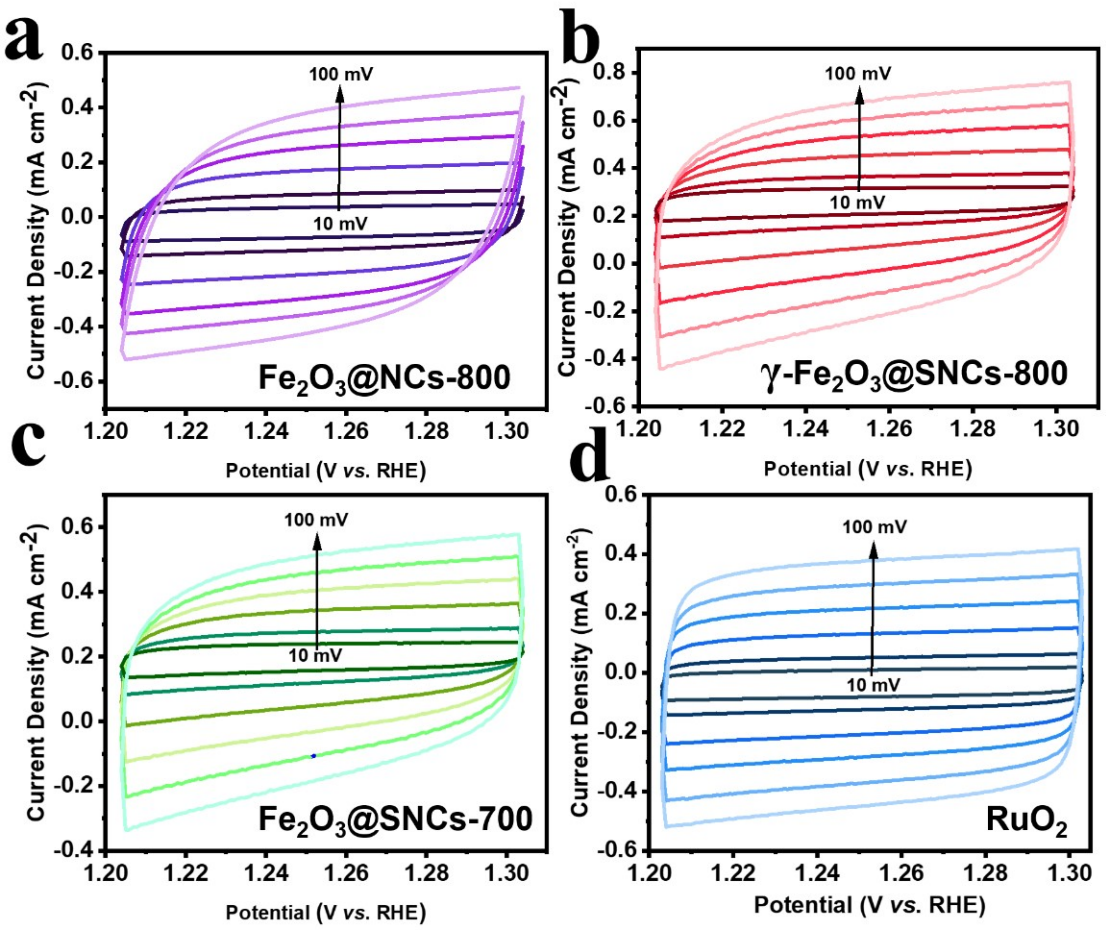

Figure S15. The CVs curves for OER C_{dl} at different scan rates of (a) Fe_2O_3@NCs-800; (b) γ-Fe_2O_3@SNCs-800; (c) Fe_2O_3@SNCs-700 and (d) RuO_2.

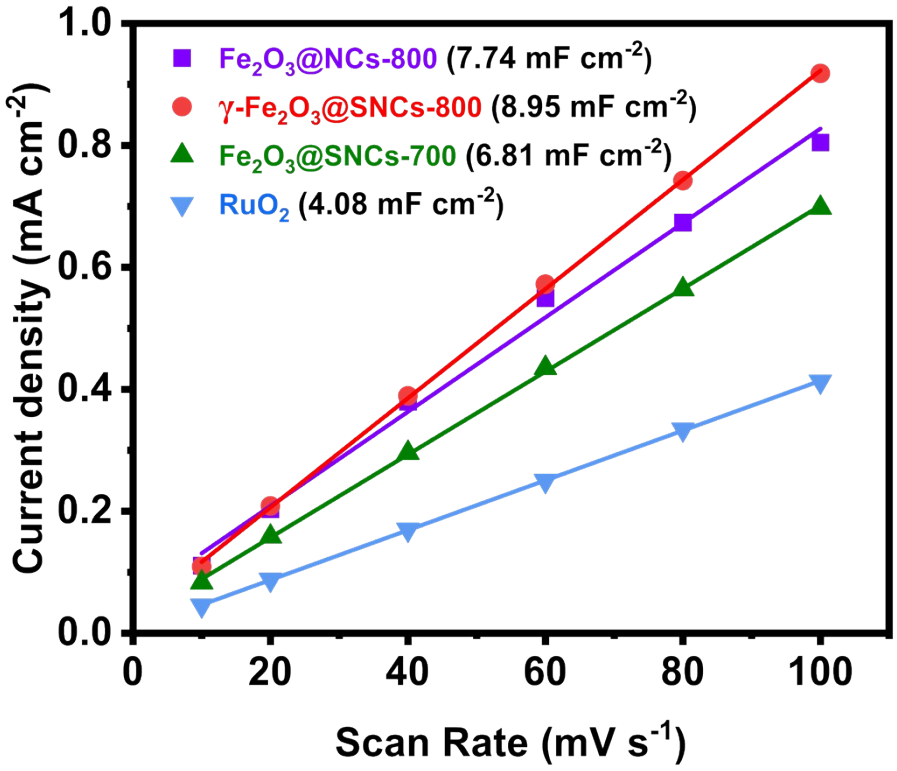

Figure S16. The linear fitting of scan rates with capacitive current densities for OER.

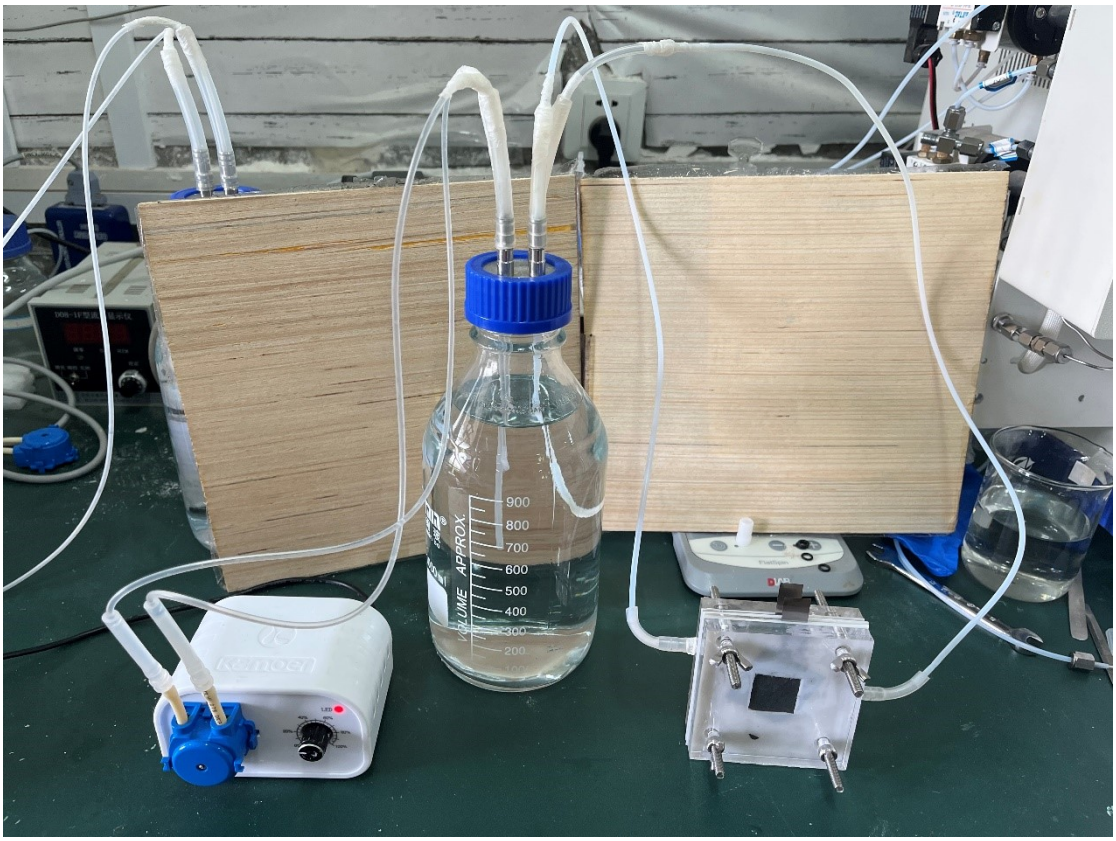

Figure S17. Device of RZAB schematic diagram.

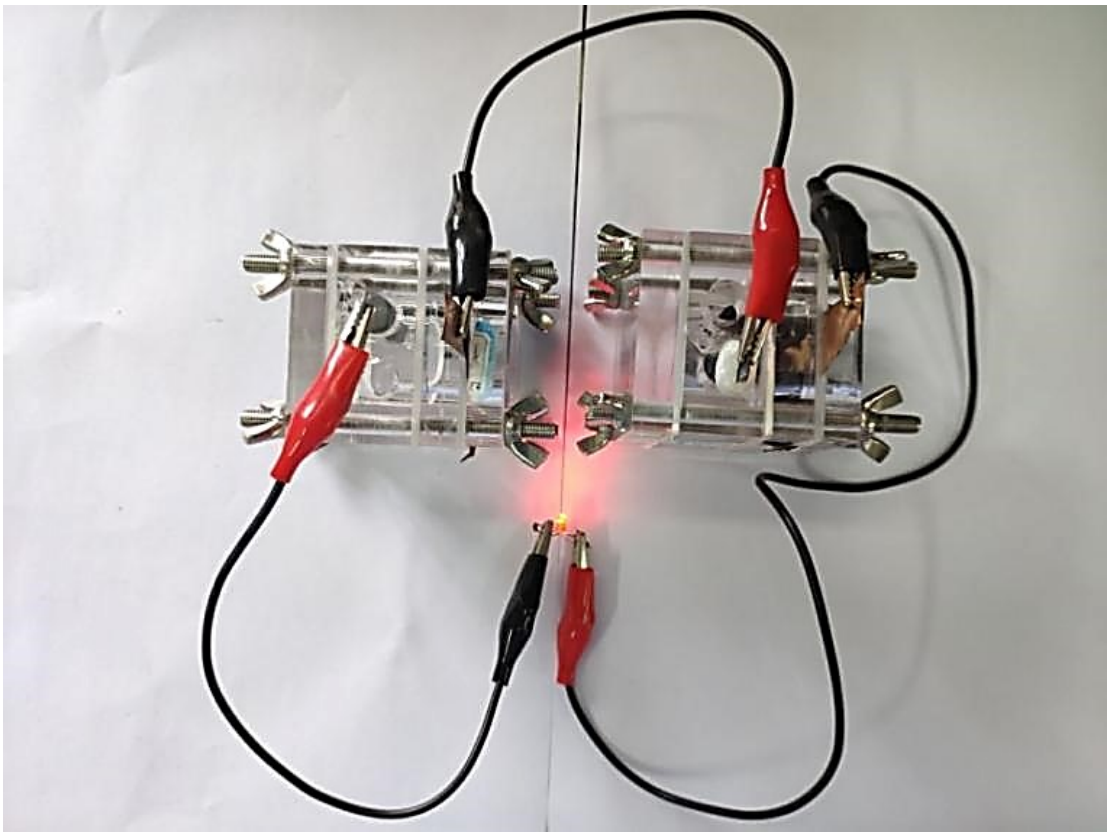

Figure S18. A lighted LED powered by two primary γ-Fe_2O_3@SNCs-800-based RZABs.

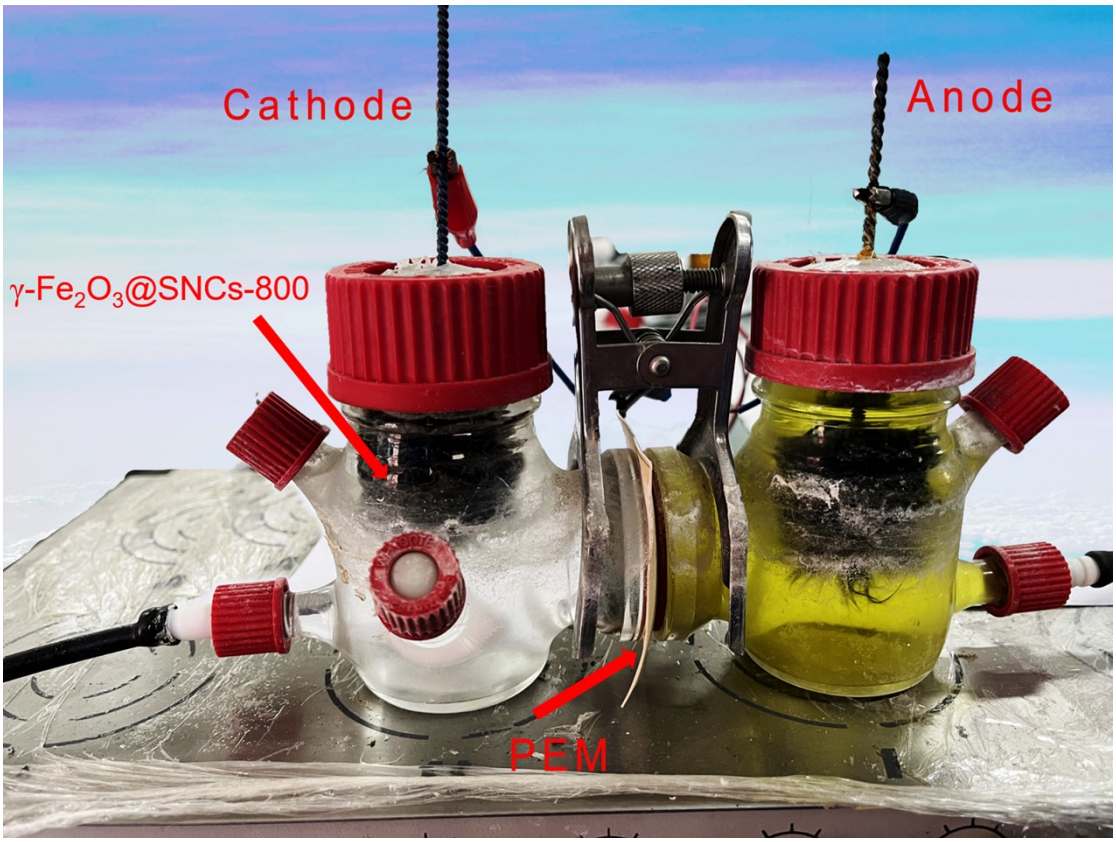

Figure S19. Device of double-chamber MFC schematic diagram.

Catalysts	Surface Area (cm^2g^{-1})	Pore Volume (cm^3g^{-1})	Pore Size (nm)
Fe_2O_3@NCs-800	268.4	0.205	4.11
γ-Fe_2O_3@SNCs-800	284.3	0.372	3.89
Fe_2O_3@SNCs-700	273.1	0.216	3.72

Table S1. Surface Area, Pore Volume, Pore Size of Fe_2O_3@NCs-800, γ-Fe_2O_3@SNCs-800, Fe_2O_3@SNCs-700.

Catalysts	$E_{j=10}$ (V)	$E_{1/2}$ (V)	ΔE (V)	Refs.
γ-Fe_2O_3@SNCs-800	**1.570**	**0.849**	**0.721**	**This work**
Fe_3O_4/CoO@CF	1.59	0.83	0.76	*Journal of Colloid and Interface Science, 2023, 640: 549-557.*
Fe,Co/DSA-NSC	1.44	0.879	0.561	*ACS Catalysis, 2023, 13(4): 2313-2325.*
Fe-Se/NC	1.623	0.925	0.698	*Angewandte Chemie International Edition, 2023: e202219191.*
RuCoOx@Co/N-CNT	1.580	0.79	0.79	*Journal of Materials Chemistry A, 2020, 8(3): 1229-1237.*
Fe/(12Zn/Co)-NCNTs	1.57	0.879	0.693	*Carbon, 2023, 205: 422-434.*
H-NSC@Co/NSC	1.60	0.85	0.75	*Small, 2022, 18(31): 2202018.*
Co_3O_4@POF	1.56	0.82	0.74	*ChemSusChem, 2020, 13(6): 1529-1536.*
CNT@SAC-Co/NCP	1.61	0.870	0.74	*Advanced Functional Materials, 2021, 31(42): 2103360.*

Table S2. Summary of some recently reported representative ORR and OER M-NC electrocatalysts in 0.1 M KOH.

Catalysts	Open circuit	Max power density	Specfic capacity	Loading (mg cm^{-2})	Refs.

	voltage (V)	(mW cm^{-2})	(mAh g^{-1})		
γ-Fe_2O_3@SNCs-800	**1.547**	**214.3**	**730.8**	**1.0**	**This work**
Fe_3O_4/N-C nanoflowers	1.457	137	740	0.2	*ACS Catalysis, 2016,6,6335*
Co-SAs@NC	1.46	105.3	897.1	0.612	*Angewandte Chemie International Edition. 2019,131,5413*
3DOM-Co@TiOxN	1.47	110	697	0.5	*Advanced Materials, 2019, 31, 1806761.*
SAC-FeN-WPC	1.53	152	735.6	0.25	*ACS Energy Letters, 2021, 6, 3624*
Enzyme-inspired Fe porphyrin	1.45	132.9	785.9	0.08	*Angewandte Chemie International Edition.2021,60,7576*
Fe_2N/Fe_7S_8, NPs	~	100.3	~	1	*J. Power Sources 2020, 457, 228038*
ZnCo/NCNTs	1.48	109.1	~	0.21	*Angewandte Chemie International Edition. 2020, 132, 6554*
Co/N@CNTs@CN MF-800	1.52	133	777	0.25	*Adv Function Materials, 2020, 30, 2003407*

Table S3. Comparison of the performance of γ-Fe_2O_3@SNCs-800-based Zn-air battery with those of catalysts reported in recent literature.

References

[1] Giannozzi P, Baroni S, Bonini N, et al.m QUANTUM ESPRESSO: a modular and open-source software project for quantum simulations of materials, *Journal of physics: Condensed matter*, 2009, **21**, 395502.

[2] Nørskov J K, Rossmeisl J, Logadottir A, et al. Origin of the overpotential for oxygen reduction at a fuel-cell cathode, *The Journal of Physical Chemistry B*, 2004, **108**, 17886-17892.

[3] Kozuch S, Martin J M L, The rate-determining step is dead. Long live the rate-determining state, *ChemPhysChem*, 2011, **12**, 1413-1418.

[4] Exner K S, Over H, Kinetics of electrocatalytic reactions from first-principles: a critical comparison with the ab initio thermodynamics approach, *Accounts of chemical research*, 2017, **50**, 1240-1247.

[5] Kozuch S, Shaik S, How to conceptualize catalytic cycles? The energetic span model, *Accounts of Chemical Research*, 2011, **44**, 101-110.

[6] Huang J, Zhang J, Eikerling M, Unifying theoretical framework for deciphering the oxygen reduction reaction on platinum, *Physical Chemistry Chemical Physics*, 2018, **20**, 11776-11786.